

Latent tri-lineage potential of adult hippocampal neural stem cells revealed by *Nf1* inactivation

Gerald J Sun^{1,2}, Yi Zhou^{1,3}, Shiori Ito¹, Michael A Bonaguidi^{1,4}, Genevieve Stein-O'Brien⁵, Nicholas K Kawasaki¹, Nikhil Modak¹, Yuan Zhu⁶, Guo-li Ming^{1-4,7} & Hongjun Song¹⁻⁵

Endogenous neural stem cells (NSCs) in the adult hippocampus are considered to be bi-potent, as they only produce neurons and astrocytes *in vivo*. In mouse, we found that inactivation of neurofibromin 1 (*Nf1*), a gene mutated in neurofibromatosis type 1, unlocked a latent oligodendrocyte lineage potential to produce all three lineages from NSCs *in vivo*. Our results suggest an avenue for promoting stem cell plasticity by targeting barriers of latent lineage potential.

It had been long postulated that continuous neurogenesis in restricted regions of the adult mammalian brain originates from tri-potent NSCs¹. Early supporting evidence includes *in vivo* observations of new neurons, astrocytes and oligodendrocytes in the subventricular zone (SVZ) of lateral ventricles and hippocampal dentate gyrus, and *in vitro* demonstrations of tri-potency of individual adult NSCs following derivation and expansion². However, recent population fate-mapping and clonal lineage-tracing of NSCs in the adult hippocampus have consistently found the generation of neurons and astrocytes, but not oligodendrocytes. In the adult SVZ, population fate-mapping studies have revealed the generation of both neurons and oligodendrocytes³, but *in vivo* clonal analysis has found only neuronal lineages⁴, and *in vitro* time-lapse analysis revealed that individual acutely isolated NPCs generate either neurons or oligodendrocytes, but never both⁵. Thus, whether NSCs with an intrinsic tri-lineage potential exist in the adult mammalian brain remains a fundamental question. How endogenous NSC lineage potential is regulated is also unknown. Incidentally, we discovered that conditional inactivation of *Nf1* in normally bi-potent radial glia-like NSCs (RGLs) in the adult dentate gyrus unlocked their latent oligodendrocytic lineage potential *in vivo*.

Mutations of *Nf1* cause neurofibromatosis type 1, a disease that is characterized by increased risk of nervous system tumorigenesis and manifestation of specific learning disabilities⁶. NF1 regulates progenitor proliferation and fate specification⁶, yet its role in NSCs in the adult hippocampus, a region critical for learning and memory, remains largely unknown. We used a tamoxifen-inducible *Nestin*^{CreERT2} mouse

line containing *loxP*-flanked (floxed) *Nf1* exons 31 and 32 and a Z/EG reporter (*Nestin*^{CreERT2}; *Nf1*^{fl/fl}; Z/EG; *Nf1*^{Nestin} mice) with multiple tamoxifen injections (Supplementary Fig. 1a,b), a model previously used to conditionally inactivate *Nf1* and identify deficits in progenitor proliferation and new neuron development in the adult hippocampus⁷. The total numbers of labeled neurons that we observed 1 month post-tamoxifen injection (mpi) in *Nf1*^{Nestin} mice were comparable to those in *Nestin*^{CreERT2}; Z/EG (control^{Nestin}) animals (Fig. 1a,b). To our surprise, in *Nf1*^{Nestin} animals, a large number of GFP⁺ cells exhibited oligodendrocyte progenitor cell (OPC) morphology and expressed NG2, but not GFAP (Fig. 1c). The presence of GFP⁺ NG2⁺ MCM2⁺ cells indicated that active proliferation of RGL-derived OPCs contributed to their final production (Supplementary Fig. 1c). Consistent with previous studies⁸⁻¹², OPCs were never observed in control^{Nestin} animals ($n = 3,564$ cells) or *Nestin*^{CreERT2}; *Nf1*^{fl/+}; Z/EG mice ($n = 2,568$ cells; Supplementary Table 1), suggesting that biallelic *Nf1* inactivation is required for OPC production. Notably, at 14 d post-tamoxifen injection (dpi), Olig2 was expressed in $10 \pm 3\%$ (mean \pm s.d.) of GFP⁺ RGLs in *Nf1*^{Nestin} mice, but was not detected in control^{Nestin} animals ($n = 3$ animals for each condition; Supplementary Fig. 1d), suggesting a potential molecular mechanism. Similar ectopic Olig2 expression was found in the adult SVZ following *Nf1* inactivation, which also leads to increased OPC production¹³. No difference in the percentage of MCM2⁺ RGLs following *Nf1* inactivation was found at 2 or 14 dpi ($n = 3$ hemispheres for each condition, $P \geq 0.4$, two-tailed unpaired *t* test).

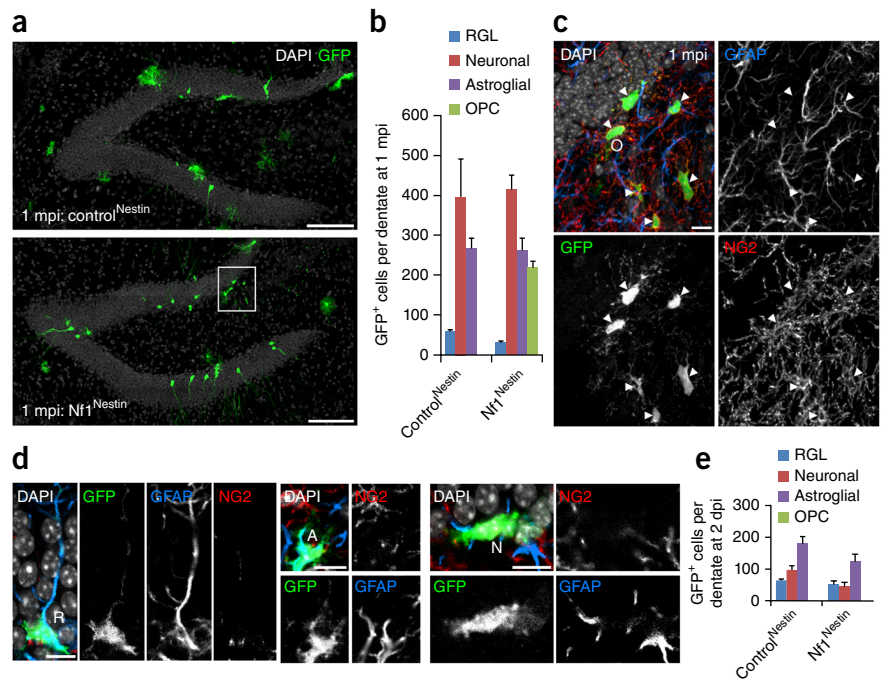
Both *Nf1* inactivation in OPCs and stress are known to induce OPC proliferation *in vivo*^{14,15}. To rule out the possibility that rare OPCs were initially labeled and became amplified, we examined *Nf1*^{Nestin} and control^{Nestin} animals at 2 dpi. No GFP⁺ OPCs were observed across the hippocampus (control^{Nestin}, $n = 1,734$ cells; *Nf1*^{Nestin}, $n = 669$ cells; Fig. 1d,e and Supplementary Table 1). Together, these data show *de novo* generation of the OPC lineage from adult NSCs that normally give rise to only neurons and astrocytes *in vivo*.

To ascertain the origin of new OPCs following *Nf1* inactivation and assess properties of individual NSCs, we performed clonal lineage-tracing of RGLs in the adult dentate gyrus (Supplementary Fig. 2a). Using a single low-dose tamoxifen injection in *Nf1*^{Nestin} or control^{Nestin} mice, we sparsely labeled, on average, 10 ± 1 precursors, including RGLs and very few intermediate neural progenitors, across the entire dentate gyrus at 2 dpi ($n = 8$ animals). No GFP⁺ OPCs were observed in any clones at 2 dpi (*Nf1*^{Nestin}, 0 of 71 clones; control^{Nestin}, 0 of 50 clones; Supplementary Table 2). At 1 or 2 mpi, we observed *Nf1*^{Nestin} clones that contained NG2⁺ cells with OPC morphology (6 of 142; Fig. 2a,b). Some clones contained astrocytes, OPCs and an RGL in close proximity (Fig. 2a and Supplementary Movie 1);

¹Institute for Cell Engineering, Johns Hopkins University School of Medicine, Baltimore, Maryland, USA. ²The Solomon H. Snyder Department of Neuroscience, Johns Hopkins University School of Medicine, Baltimore, Maryland, USA. ³Biochemistry, Cellular and Molecular Biology Graduate Program, Johns Hopkins University School of Medicine, Baltimore, Maryland, USA. ⁴Department of Neurology, Johns Hopkins University School of Medicine, Baltimore, Maryland, USA. ⁵Pre-doctoral Human Genetics Training Program, Johns Hopkins University School of Medicine, Baltimore, Maryland, USA. ⁶Gilbert Family Neurofibromatosis Institute, Center for Cancer and Immunology Research, Children's National Medical Center, Washington, DC, USA. ⁷Department of Psychiatry and Behavioral Sciences, Johns Hopkins University School of Medicine, Baltimore, Maryland, USA. Correspondence should be addressed to H.S. (shongju1@jhmi.edu) or G.M. (gming1@jhmi.edu).

Received 17 June; accepted 6 October; published online 2 November 2015; doi:10.1038/nn.4159

Figure 1 *Nestin^{CreERT2}*-based conditional *Nf1* inactivation in adult hippocampal neural progenitors leads to generation of oligodendrocyte progenitor cells. (a) Sample projected confocal images in the population-labeling procedure at 1 mpi in control^{Nestin} (top) and *Nf1^{Nestin}* (bottom) animals. (b) Quantification of total GFP⁺ cell numbers by lineage across the dentate gyrus at 1 mpi. Data are presented as mean \pm s.e.m. (c) High-magnification projected confocal images of the boxed region in (a). Filled arrowheads denote GFP⁺ NG2⁺ GFAP⁻ OPCs (O). (d) Representative GFP⁺ cells at 2 dpi include RGLs (R), astrocytes (A) and newborn intermediate neural progenitor cells (N) in *Nf1^{Nestin}* animals. (e) Quantification of total GFP⁺ cell numbers by lineage across the dentate gyrus at 2 dpi. Data are presented as mean \pm s.e.m. Scale bars represent 100 μ m (a) and 10 μ m (c,d). See **Supplementary Table 1** for the numbers of animals examined under different conditions.



other clones lacked RGLs, potentially as a result of RGL differentiation¹⁰ or death (Fig. 2b). Consistent with our previous characterization of RGLs in multiple clonal lineage-tracing studies^{10–12} (over 504 clones in total), we found no OPCs in any of the control^{Nestin} clones (0 of 116; **Supplementary Table 2**). Some RGLs with four rounds of cell division still did not generate OPCs in control^{Nestin} animals (Fig. 2c). Most *Nf1^{Nestin}* clones (136 of 142) did not produce OPCs (Fig. 2d), which could have been a result of incomplete recombination of reporter and both *Nf1* floxed alleles in the same cell following a single low-dose tamoxifen induction, and/or *Nf1* inactivation only unlocking the potential for, but not restricting, the RGL fate to OPCs, as shown in population fate mapping (Fig. 1). Notably, the size of

Nf1^{Nestin} clones with OPCs was larger than those of control^{Nestin} at 1 mpi (**Supplementary Fig. 2b**). Consistent with a previous report⁷, some *Nf1^{Nestin}* clones at 1 or 2 mpi contained mis-positioned labeled neurons, indicative of successful *Nf1* inactivation in at least some of labeled clones. Notably, some neurons in *Nf1^{Nestin}* clones migrated into the molecular layer (**Supplementary Fig. 2c**), suggesting a critical role for NF1 in regulating the migration of newborn neurons during adult neurogenesis.

We validated our finding by clonal analysis using an independent tamoxifen-inducible *Gli1^{CreERT2}* line that also specifically targets RGLs in the adult dentate gyrus¹⁶. We generated two mouse lines: *Gli1^{CreERT2}*; *Nf1^{fl/fl}*;

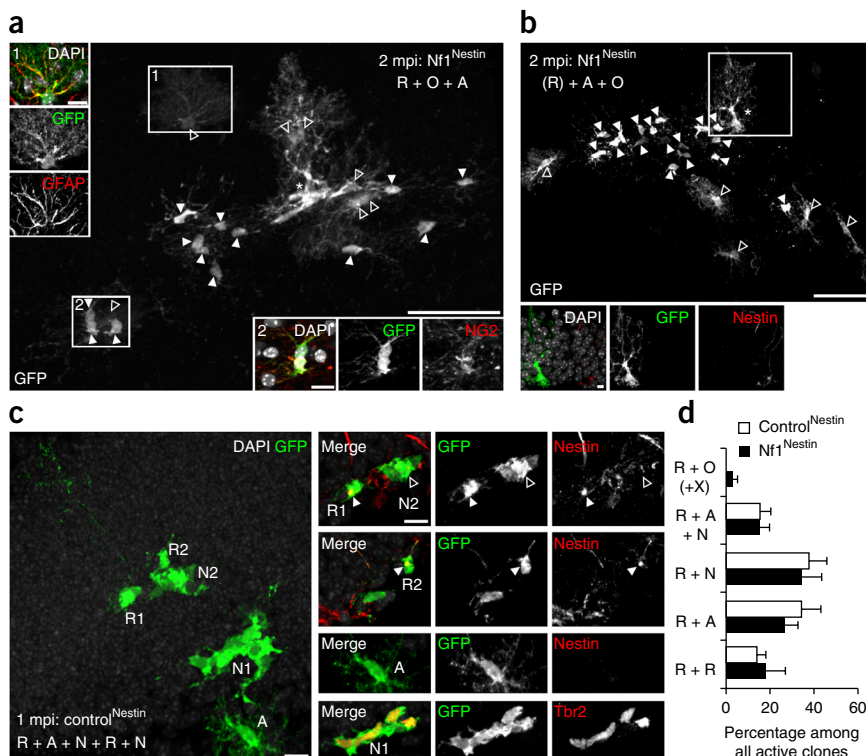


Figure 2 Clonal lineage-tracing of RGLs following conditional *Nf1* inactivation reveals RGLs as OPC cell of origin. (a) A clone at 2 mpi in *Nf1^{Nestin}* mice with a maintained RGL (R, *), OPCs (O, filled arrowheads; see example in inset 2) and astrocytes (A, open arrowheads; see example in inset 1). Scale bars represent 50 μ m and 10 μ m (inset). (b) A clone at 2 mpi in a *Nf1^{Nestin}* animal with differentiated RGL (*), OPCs (filled arrowheads) and astrocytes (open arrowheads). Inset, the differentiated RGL still possessed radial morphology, but lacked expression of nestin. Scale bars represent 50 μ m and 10 μ m (inset). (c) A clone at 1 mpi in a control^{Nestin} animal with maintained RGL (R1, R2) that underwent at least three rounds of division to symmetrically self-renew into two nestin⁺ RGLs (R1, R2), generated two distinct clusters of Tbr2⁺ newborn intermediate neural progenitor cells (N1, N2), and a nestin⁻ astrocyte (A). Scale bars represent 10 μ m. (d) Quantitative comparison of the frequency of different RGL fate choices observed at 1 mpi. X represents A, N, or A + N. Data are presented as mean \pm s.e.m. See **Supplementary Table 2** for number of hemispheres examined under different conditions.

Z/EG (Nf1^{Gli1}) and *Gli1*^{CreERT2}; Z/EG (control^{Gli1}; **Supplementary Fig. 3a**). No GFP⁺ OPCs were observed at 2 dpi (Nf1^{Gli1}, 0 of 20 clones; control^{Gli1}, 0 of 34 clones; **Supplementary Table 3**). At 1 mpi, we observed OPC-containing clones in Nf1^{Gli1} animals (8 of 68 clones), but never in control^{Gli1} animals (0 of 38 clones; **Supplementary Fig. 2b,c** and **Supplementary Table 3**). Notably, some clones at 1 mpi in Nf1^{Gli1} animals contained three lineages: neurons, astrocytes and OPCs (3 of 68 clones; **Supplementary Fig. 3b**). Together, these results suggest that RGLs in the adult hippocampus possess an intrinsic ability to generate all three major neural lineages, and the OPC lineage potential is actively restricted by NF1.

The concept of adult NSCs with a defining trait of multi-lineage neuronal, astrocytic and oligodendrocytic potential was established over two decades ago¹, yet no endogenous tri-potent NSCs have been shown. In the current model, NSCs are gradually specified during development and become restricted in their lineage potential in adult¹⁷; they can only regain the tri-potentiality *in vitro* after removal from their local environment and treatment with growth factors. Our results suggest a new model in which adult NSCs are intrinsically tri-potent and their fate specification is regulated not only by positive instructive cues, but also by inhibitory signaling that actively suppresses certain fates (**Supplementary Fig. 4**). As NF1, a cytoplasmic regulator of Ras and cAMP signaling⁶, is neither a transcription factor nor a known direct reprogramming factor, our model is conceptually different from reprogramming, for example, in the case of a neuronal to oligodendrocytic fate switch following forced *Ascl1* overexpression in proliferating hippocampal neural progenitors¹⁸. *Nf1* inactivation does not convert RGLs to OPCs, as other fates are still produced. Instead, our result supports an emerging view that latent lineage potentials could be actively suppressed in precursors or even in apparently differentiated cell types. For example, adult striatal astrocytes were recently shown to exhibit a latent neurogenic program that is actively suppressed by Notch signaling¹⁹ and can be elicited by injury²⁰. This new framework enriches our understanding of fundamental stem cell biology and opens new avenues for stem cell plasticity or therapeutics via targeting barriers of a cell's intrinsic lineage potential.

METHODS

Methods and any associated references are available in the [online version of the paper](#).

Note: Any Supplementary Information and Source Data files are available in the online version of the paper.

ACKNOWLEDGMENTS

We thank members of the Ming and Song laboratories for discussion, and Y. Cai and L. Liu for technical support. This work was supported by the US National Institutes of Health (NS047344 to H.S., NS080913 to M.A.B., and NS048271 and MH105128 to G.M.), and by a pre-doctoral fellowship from The Children's Tumor Foundation to G.J.S.

AUTHOR CONTRIBUTIONS

G.J.S., H.S. and G.M. designed the project. G.J.S. contributed to all aspects of the study. Y. Zhou, S.I., G.S.-O'B., N.K.K. and N.M. performed the experiments. M.A.B. provided some initial data. Y. Zhu contributed reagents. G.J.S., H.S. and G.M. wrote the manuscript.

COMPETING FINANCIAL INTERESTS

The authors declare no competing financial interests.

Reprints and permissions information is available online at <http://www.nature.com/reprints/index.html>.

- Gage, F.H. *Science* **287**, 1433–1438 (2000).
- Ming, G.L. & Song, H. *Neuron* **70**, 687–702 (2011).
- Menn, B. *et al. J. Neurosci.* **26**, 7907–7918 (2006).
- Calzolari, F. *et al. Nat. Neurosci.* **18**, 490–492 (2015).
- Ortega, F. *et al. Nat. Cell Biol.* **15**, 602–613 (2013).
- Gutmann, D.H., Parada, L.F., Silva, A.J. & Ratner, N. *J. Neurosci.* **32**, 14087–14093 (2012).
- Li, Y., Li, Y., McKay, R.M., Riethmacher, D. & Parada, L.F. *J. Neurosci.* **32**, 3529–3539 (2012).
- Lagace, D.C. *et al. J. Neurosci.* **27**, 12623–12629 (2007).
- Dranovsky, A. *et al. Neuron* **70**, 908–923 (2011).
- Bonaguidi, M.A. *et al. Cell* **145**, 1142–1155 (2011).
- Song, J. *et al. Nature* **489**, 150–154 (2012).
- Jang, M.H. *et al. Cell Stem Cell* **12**, 215–223 (2013).
- Wang, Y. *et al. Cell* **150**, 816–830 (2012).
- Liu, C. *et al. Cell* **146**, 209–221 (2011).
- Chetty, S. *et al. Mol. Psychiatry* **19**, 1275–1283 (2014).
- Ahn, S. & Joyner, A.L. *Nature* **437**, 894–897 (2005).
- Kriegstein, A. & Alvarez-Buylla, A. *Annu. Rev. Neurosci.* **32**, 149–184 (2009).
- Jessberger, S., Toni, N., Clemenson, G.D. Jr., Ray, J. & Gage, F.H. *Nat. Neurosci.* **11**, 888–893 (2008).
- Magnusson, J.P. *et al. Science* **346**, 237–241 (2014).
- Nato, G. *et al. Development* **142**, 840–845 (2015).

ONLINE METHODS

Animals and tamoxifen administration. *Nestin^{CreERT2}; Nf1^{f/f}; Z/EG^{f/f}-*, *Nestin^{CreERT2}; Nf1^{f/+}; Z/EG^{f/f}-*, and *Nestin^{CreERT2}; Z/EG^{f/f}-* mice were generated by crossing *Nestin^{CreERT2}* driver²¹ with *Z/EG^{f/f}* reporter²² (Tg(CAG-Bgeo/GFP)21Lbe/J, Jackson Labs) and *Nf1^{f/f}* mice²³, where applicable. *Gli1^{CreERT2}; Nf1^{f/f}; Z/EG^{f/f}-* and *Gli1^{CreERT2}; Z/EG^{f/f}-* mice were generated in a similar fashion, but with *Gli1^{CreERT2}* mice¹⁶. All mice in the study were backcrossed to the C57BL/6 background for at least six generations. Animals were housed in a 14-h light/10-h dark cycle and had free access to food and water. Tamoxifen (66.67 mg/ml, Sigma, T5648) was prepared in a 5:1 corn oil (Sigma) to ethanol mixture. As a result of differences in CreERT² mouse generation, different tamoxifen injection procedures were required to enable sparse labeling for clonal analysis (~8–16 clones per hemisphere). A single 62.5 mg per kg of body weight dose of tamoxifen (for *Nestin^{CreERT2}*) or a 125 mg per kg dose every 12 h for 4 total doses (for *Gli1^{CreERT2}*) was intraperitoneally injected into adult 8–10 week-old male and female mice (**Supplementary Table 4**). For population cell labeling in *Nestin^{CreERT2}*, animals were injected with 125 mg per kg every 12 h 4 times (**Supplementary Table 4**). Animals were analyzed at 2 dpi, 14 dpi, or 1–2 mpi. For animals with multiple injections, dpi and mpi were counted starting from the final injection. All animal procedures were performed in accordance to institutional guidelines of Johns Hopkins University School of Medicine.

Tissue processing, immunostaining and confocal imaging. Animals were transcardially perfused with cold 4% paraformaldehyde (wt/vol, in 0.1 M phosphate buffer, PB, pH 7.4), and cryoprotected with 30% sucrose (wt/vol). Serial 40- μ m-thick coronal brain sections were cut on a frozen sliding microtome (Leica, SM2010R) for immunohistology as previously described^{10,24}. Antibodies diluted in TBS with 0.05% Triton X-100 (vol/vol) and 3% donkey serum (vol/vol), were used against GFP (Aves Labs, GFP-1020, chicken, 1:500; Rockland, 600-101-215, goat, 1:500; AbD Serotec, 4745-1051, sheep, 1:500), Tbr2 (Abcam, ab23345, rabbit, 1:250), GFAP (Millipore, MAB360, mouse, 1:1,000; DAKO, Z033401-2, rabbit, 1:1,000), Nestin (Aves Labs, NES, chicken, 1:500), Prox1 (Millipore, MAB5654, mouse, 1:500), NG2 (Millipore, AB5320, rabbit, 1:200), Olig2 (a generous gift from B. Novitsch (University of California, Los Angeles), guinea pig, 1:20,000). Nestin antigen was retrieved by incubating brain sections in 1 \times DAKO target retrieval solution (DAKO) at 68 °C for 20 min, followed by 10 min cooling to at 20 °C. Serial sections from the entire dentate gyrus were first immunostained for GFP to allow

identification of prospective clone-containing sections on an epifluorescence microscope (Zeiss, Axiovert 200M). Labeled clone-containing sections were taken for further processing and confocal imaging at 40 \times on a Zeiss LSM 710 confocal microscope using multi-track or spectral linear unmixing 'online fingerprinting' configurations (Carl Zeiss).

Image processing and data analyses. For population cell labeling experiments, cells were counted manually by visualizing the serial dentate gyrus sections on an epifluorescence microscope. Due to the difficulty in reliably quantifying small, densely packed transient-amplifying neural progenitors, only cells with mature neuron morphology were counted as belonging to the neuronal lineage at 1 mpi. For clonal cell labeling experiments, identification of clones amongst GFP-labeled clusters of cells was performed as previously described^{10,25}. Clones that spanned multiple serial sections were reconstructed using Reconstruct software as previously described^{10,25}. All aligned images were exported at full resolution for three-dimensional visualization into Imaris (Bitplane) and analyzed. All other confocal images were directly visualized and analyzed in Imaris. Movie of three-dimensional-rendered clone was generated using the Animation feature in Imaris. Clones were analyzed in a dentate gyrus volume that included the molecular layer, granule cell layer, subgranular zone, and hilus, excluding the polymorphic layer (CA4) protruding into the posterior dentate gyrus. Clonal cell fate frequencies were calculated per brain hemisphere and averaged across hemispheres. Numbers of cells and animals counted and used, respectively, are shown in **Supplementary Tables 1–3**. No statistical methods were used to pre-determine sample sizes; sample sizes were similar to those reported in previous studies^{10,11}. Due to the binary nature of the reported phenomenon, randomization and blinding were not employed. A two-sample Kolmogorov–Smirnov test was used to statistically compare clone cell number distributions. A two-sample unpaired Student's *t* test was used to statistically compare the percentage of MCM2⁺ RGLs upon *Nf1* inactivation at 2 or 14 dpi.

A **Supplementary Methods Checklist** is available.

21. Balordi, F. & Fishell, G. *J. Neurosci.* **27**, 14248–14259 (2007).

22. Novak, A., Guo, C., Yang, W., Nagy, A. & Lobe, C.G. *Genesis* **28**, 147–155 (2000).

23. Zhu, Y. *et al. Genes Dev.* **15**, 859–876 (2001).

24. Berg, D.A. *et al. Front. Biol.* **10**, 262–271 (2015).

25. Sun, G.J. *et al. Proc. Natl. Acad. Sci. USA* **112**, 9484–9489 (2015).